Dynamic Multiphase Bidirectional EV On-Board Charger Using Fuzzy Logic Control for Wide Power and Voltage Ranges

Dokkari Gopichand[1], S.Rajendra Prasad[2], R.S.R.Krishnam Naidu[3]
[1]*M.Tech Student, Department of Electrical and Electronics Engineering, Nadimpalli Satyanarayana Raju Institute of Technology(A), Sontyam, Visakhapatnam, India*
[2]*Assistant Professor, Department of Electrical and Electronics Engineering, Nadimpalli Satyanarayana Raju Institute of Technology(A), Sontyam, Visakhapatnam, India*
[3]*Professor Department of Electrical and Electronics Engineering, Nadimpalli Satyanarayana Raju Institute of Technology(A), Sontyam, Visakhapatnam, India*

Abstract -Modern electric vehicles depend on advanced power electronics like on-board chargers (OBCs) and DC–DC converters that must operate reliably under varying conditions, including phase number, input voltage, and battery output levels. Achieving high efficiency and low cost while meeting automotive standards is increasingly complex. This article introduces a novel OBC architecture that maintains full power output across both single-phase and three-phase inputs—without additional power components or performance trade-offs. Central to this design is the use of fuzzy control, enabling adaptive, efficient operation under fluctuating conditions. The result is a compact, high-efficiency, and cost-effective universal charging solution.

I. OVERVIEW

Electric vehicles (EVs) play a vital role in electrification and decarbonization, with batteries serving as the core energy source for driving electric motors and onboard systems. EVs typically support two types of power inputs: a fast-charging DC port delivering 50–350 kW for rapid charging, and a low-power AC port (6.6–22 kW) for flexible charging from standard grid outlets. The on-board charger (OBC), or converter, handles two key functions: adapting to various grid configurations (single-, split-, or three-phase at 85–265V and 40–65 Hz) and ensuring electrical isolation and voltage regulation for safety. Recent studies have highlighted the importance of highly adaptable OBCs capable of wide voltage and power operation, with growing interest in multiphase and bidirectional systems.

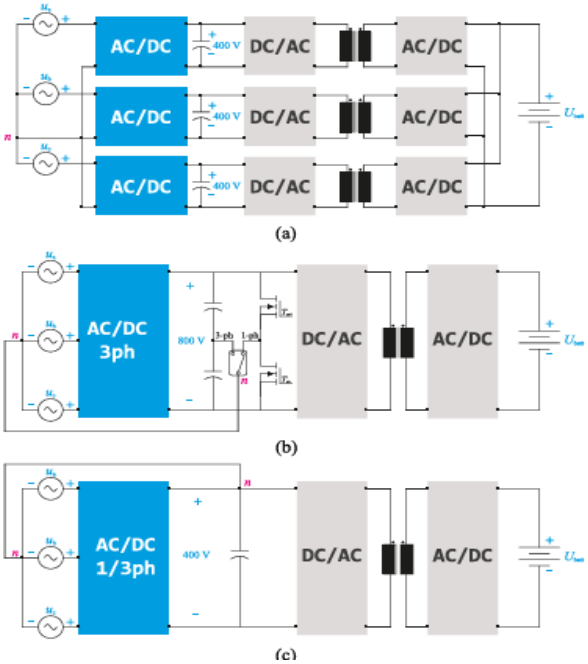

FIGURE 1. Bidirectional OBC charger architectures achieving a unity power factor consist of an ac–dc front-end and a back-end isolated dc–dc converter. (a) Phase modular (3×400V) and (b) single (800V) front-end stage architectures that convert three-phase ac voltages ua, ub, uc (or conversely, a single-phase voltage uabc) to an isolated dc output voltage Ubatt. (c) Proposed single-/three-phase single-front-end stage achieving 400V output voltage.

To meet modern OBC demands, a typical solution is a two-stage converter with power factor correction (PFC) and isolated DC–DC conversion, often using a 400V battery and optimized 600V semiconductor tech. While bidirectional designs like totem-pole rectifiers are feasible, operating in three-phase mode requires multiple power rails, isolated transformers, and complex control and sensing systems—driving up cost and reducing efficiency and power density.

Switching to a three-phase rectifier with a single DC–DC stage simplifies the design and improves power density. The rise of 1200V SiC devices and 800V batteries has further enabled high-efficiency, bidirectional OBCs suitable for vehicle-to-home, vehicle-to-load, and vehicle-to-vehicle use cases. However, current architectures struggle with wide input/output variations and require extra components in single-phase modes, leading to reduced efficiency and more complex circuitry—especially due to high intermediate DC-link voltages (750–850V) that exceed electrolytic capacitor ratings. To address these challenges, this article proposes a compact and cost-effective OBC using integrated single-phase rectifiers with a common ground reference. This architecture supports seamless single-/three-phase operation without extra power devices, enabling the use of 400V DC-link and standard electrolytic capacitors. A full-bridge dual-active bridge (DAB) stage ensures bidirectional power flow, voltage regulation, and isolation. The rest of the article outlines the architecture (Section II), control method (Section III), design equations (Section IV), and results (Section V).

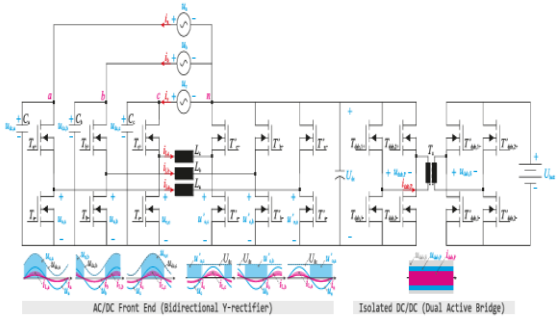

FIGURE 2. Proposed bidirectional OBC architecture in three-phase operation including the main high-frequency waveforms during a grid cycle.

2. Principle of Operation

A. Proposed Converter

The converter uses a two-stage architecture to deliver flexibility in handling wide battery voltage ranges, grid fluctuations, and to ensure isolation. The first stage is a bidirectional single-/three-phase AC–DC front-end, designed for efficient grid power interface. The second stage is an isolated Dual Active Bridge (DAB) DC–DC converter, which manages voltage conversion and provides galvanic isolation. Figure 2 shows the converter setup and its waveforms under three-phase operation.

B. AC–DC Front-End

A differential rectifier based on the phase-modular buck-boost Y-rectifier concept is proposed. Each of the three input phases uses a buck-boost DC–DC converter tied to a common star (Y) point connected to the positive DC-link (UDC). This setup ensures balanced voltage and current stress in both single- and three-phase modes.

Each phase consists of:

A DC-side half-bridge connected to the positive DC rail (and grid neutral),

An AC-side half-bridge connected to the respective grid terminal (a, b, or c).

This arrangement allows for seamless operation in both single- and three-phase modes using simple relay-based reconfiguration, without increasing component count. In three-phase mode, phase voltages (ua, ub, uc) are applied to terminals (a, b, c), and the converter draws sinusoidal currents (ia, ib, ic) that are in phase with these voltages.

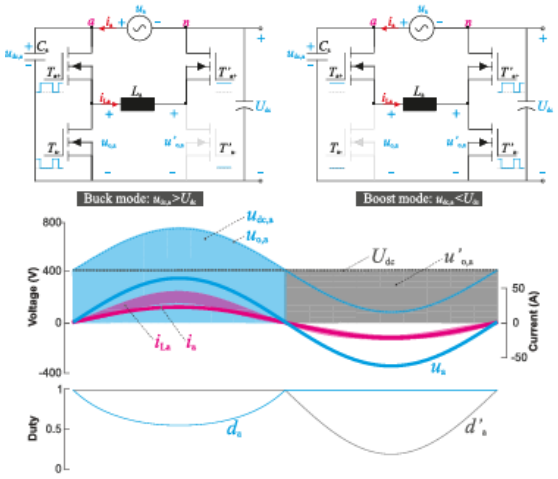

FIGURE 3. Operating modes of the ac–dc front-end module a (top), and corresponding converter waveforms (middle), and modulation parameters (bottom).

This converter operates uniformly across all phases. For simplicity, its operation is described for phase a, as shown in Fig. 3; the same process applies to the other phases. The system is built around the UDC rail and uses a half-bridge leg on both the AC and DC sides per phase—labeled Ta^{+} and Ta^{-}.

A key advantage of this design is its ability to support both single-phase and three-phase operation without additional components. Relay-based reconfiguration enables this flexibility. During operation, the converter generates sinusoidal grid

currents (ia, ib, ic) that are in phase with the corresponding grid voltages. Each grid cycle is divided into two complementary modes, allowing efficient and balanced operation within a single grid period.

a) Mode I: In this mode, the AC-side half-bridge transistors Ta^+ and Ta^- are switched complementarily. Ta^+ remains ON when the grid voltage is positive (ua > 0). Since the grid frequency (f_ac) is much lower than the converter's switching frequency (f_sw), the equivalent duty cycle of the AC-side half-bridge (d_a) can be defined accordingly.

$$d_a(t) = \{\frac{U_{dc}}{U_{dc}+U_a(t)} \; U_a \geq 0 \; 1, \; U_a > 0 \quad (1)$$

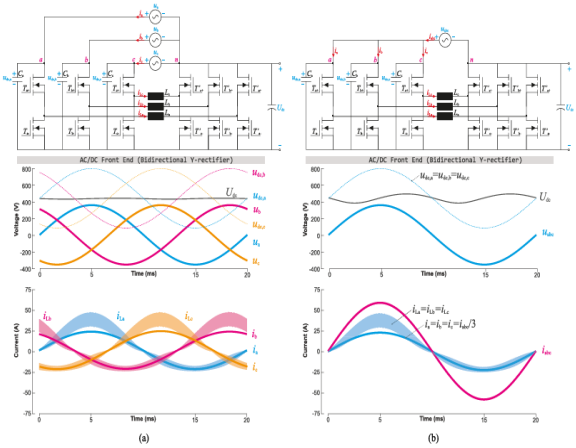

FIGURE 4. Proposed bidirectional OBC architecture including the main grid voltage and current waveforms for (a) three-phase operation and (b) single-phase operation.

When the grid-phase voltage (ua) combines with the intermediate DC-link voltage (Udc), it results in the AC-side half-bridge input capacitor voltage:
udc,a = Udc + ua.
To ensure proper operation across a wide grid voltage range (Uac = 85–265 V_{RMS}), this capacitor voltage (udc,a) must remain strictly positive (udc,a > 0). This requirement sets the intermediate DC-link voltage to Udc = 400–450 V.

As a result, whether operating in single-phase or three-phase mode:
600 V-rated power devices are sufficient for the DC-side half-bridge legs, while 1200 V-rated SiC MOSFETs are required for the AC-side half-bridge legs, due to the maximum voltage stress:
Udc,a,max = Udc + Ua,pk = 520–825 V.

$$d_a(t) = \{1, \; U_a \geq 0 \; \frac{U_{dc}}{U_{dc}+U_a(t)}, U_a > 0 \quad (2)$$

The applied duty cycles that produce a mutually exclusive high-frequency switching activity are displayed in Fig. 3. Just three of the six half-bridges are switched simultaneously across the entire ac–dc front-end due to the ac- and dc-stages. As a result, switching losses are considerably decreased. The suggested converter, in contrast to the phase modular buck-boost Y-rectifier [22], advantageously connects the intermediate dc-link bus, Udc, with the grid neutral point n. This suggests that in the event of a single-phase connection [see Fig. 4(b)], the parallel-connected ac-side terminals a, b, and c are connected to the grid voltage uabc in order to distribute the current evenly among the phase modules. The single-phase grid current iabc has a return path thanks to the previously indicated connection between the grid neutral point and the positive intermediate dc-link. One of the primary benefits of the suggested converter over earlier models is that it enables full output power range operating in both single-phase and three-phase operation without requiring extra components or oversizing power devices. Additionally, the control architecture and isolation considerations are made simpler by the fact that the ac- and dc-side half-bridge legs are referenced to the same point

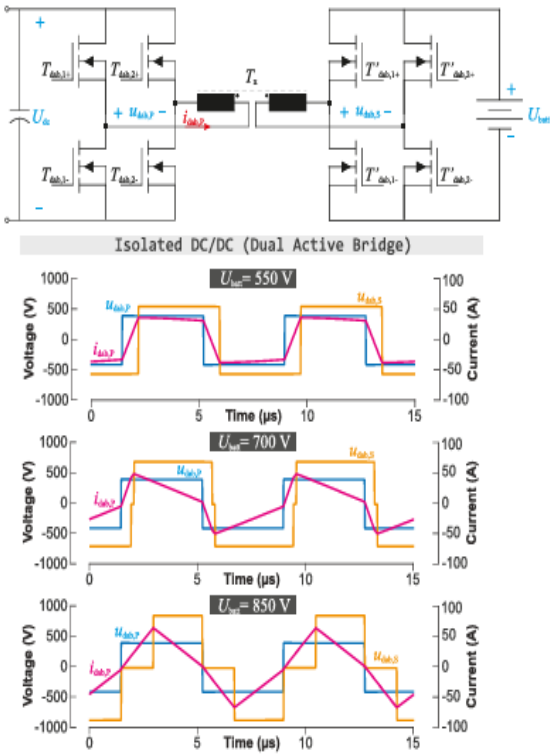

FIGURE 5. Operating modes of the dc–dc back-end module a (top), and corresponding converter waveforms (bottom).

C. DC-DC Converter DAB

The rear stage of the proposed OBC system incorporates a single Dual Active Bridge (DAB) DC–DC converter, which provides galvanic isolation through a high-frequency transformer. This converter consists of full-bridge circuits on both the primary and secondary sides, using a modulation strategy that supports bidirectional power transfer and adapts to varying battery voltage levels. By employing a single isolated DC–DC stage, the design reduces the number of power devices and magnetic components, thereby simplifying the overall control and isolation architecture compared to modular approaches [see Fig. 1(a)]. The transformer's optimal turns ratio has been determined as n = 1.34, enabling efficient voltage conversion from the 400 V intermediate DC-link to a wide battery voltage range typical of 800 V systems (Ubatt = 550–850 V). Under heavy load conditions—such as during low battery voltage—the system operates in pseudo-trapezoidal mode to reduce conduction losses. Additionally, full Zero Voltage Switching (ZVS) is achieved on both bridges to enhance efficiency. In the medium-to-high battery voltage range, secondary-side duty cycle modulation is employed to refine the modulation profile and minimize power losses, as detailed in [23]. These modulation behaviors are illustrated in Fig. 5.

III. STRATEGY FOR CONTROL

To function effectively in a range of conditions, ensuring sinusoidal input current consumption and a smooth battery. As of right moment, three control loops are in place. These loops ensure the converter works as intended by maintaining a constant battery current, either positive or negative, fed by a scaled mains-voltage current level and, consequently, in phase with the mains voltage (see Fig. 6). An AMD/Xilinx field programmable gate array (FPGA) serves as the digital control platform, ensuring accurate control loop execution and precise pulsewidth modulation production. First, "Control Loop A" balances the battery's and mains' power consumption by using the dc-link capacitor voltage stabilization. The dc-link voltage Udc is measured twice during each mains cycle, and its peak value, Udc,peak, is calculated.

To maintain the required mains RMS current level Iac,rmsI_{ac,rms}Iac,rms and balance power consumption, the PI controller operates at both positive and negative zero crossings of the mains waveform. Control Loop B ensures that the instantaneous mains current remains in phase with the mains voltage. At the end of each switching period, this loop runs three identical modules—one for each phase—in parallel. The duty cycles for the rectifier's buck-boost stages are calculated by combining the output of the MATH unit (which computes expressions (1) and (2)) with the output of the PI controller. This coordinated process ensures the correct instantaneous mains current. Control Loop C, the third loop, is responsible for maintaining the desired battery current level Ibat,OBJI_{bat,OBJ}Ibat,OBJ.

To accommodate variations in the DC-link voltage and ensure the battery receives a consistent current, a PI controller is executed once per switching cycle. The DAB LUT (Dual Active Bridge Lookup Table) is employed to determine the optimal modulation strategy. This selection is based on key input parameters, including the battery voltage, DC-link voltage, and the required gain KDABK_{DAB}KDAB.

IV. FUZZY LOGIC CONTROLLER (FLC)

Fuzzy Logic Controller (FLC) is an advanced control strategy that mimics human reasoning to handle uncertain and imprecise data, making it highly suitable for complex and nonlinear systems where traditional control methods struggle. Unlike classical binary logic, which operates strictly on true or false values (1 or 0), fuzzy logic introduces a degree of flexibility by allowing values between 0 and 1, representing partial truths. This capability enables FLCs to process linguistic variables like "high," "medium," or "low," making them ideal for real-world applications where precision is difficult to define. The working of a fuzzy logic controller consists of four primary stages: fuzzification, rule base, inference engine, and defuzzification. The first stage, fuzzification, involves converting crisp numerical inputs into fuzzy values using membership functions, which define how each input belongs to different fuzzy sets.

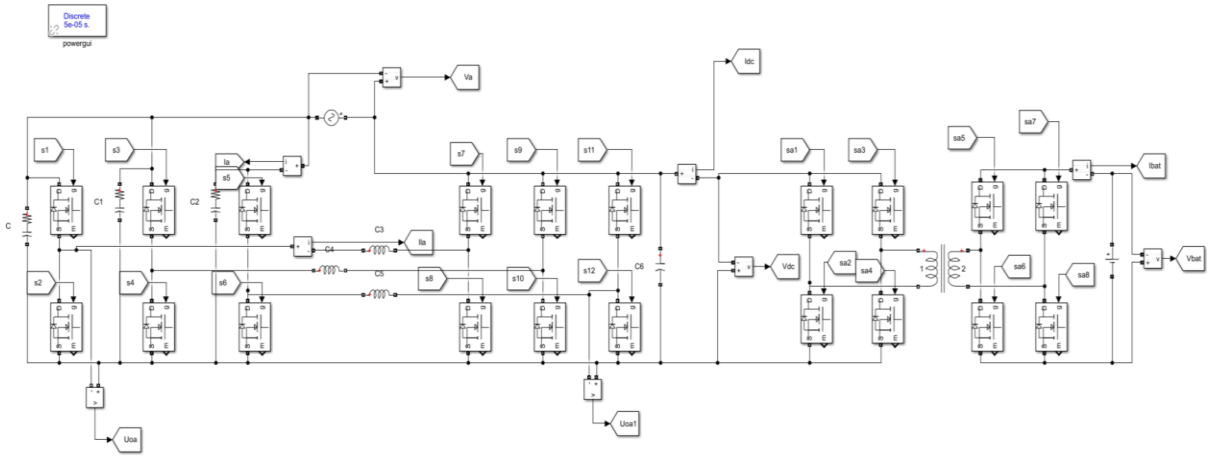

Fig 6: Single buck–boost cell operation for Uac = 230 circuit diagram of Bidirectional of ev on boarding charging These membership functions can take various forms, such as triangular, trapezoidal, or Gaussian, depending on the system's requirements. Once the inputs are fuzzified, the rule base comes into play, consisting of a set of IF-THEN rules that define the system's behaviour.

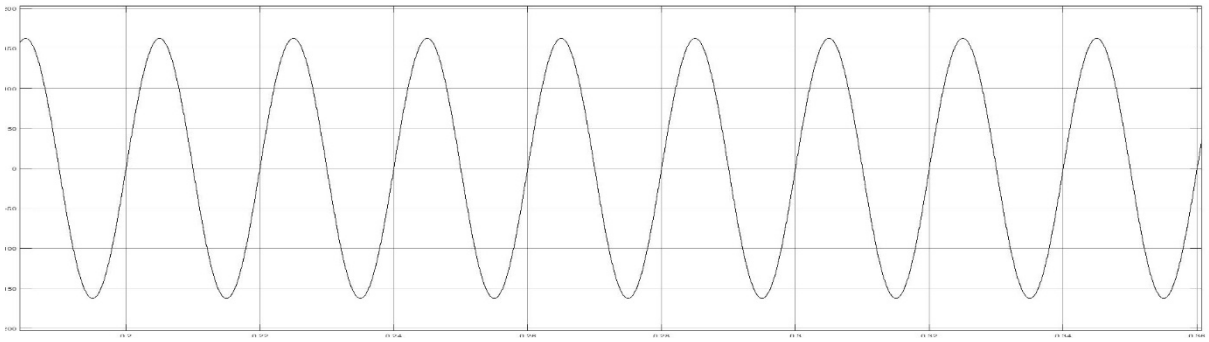

(a)

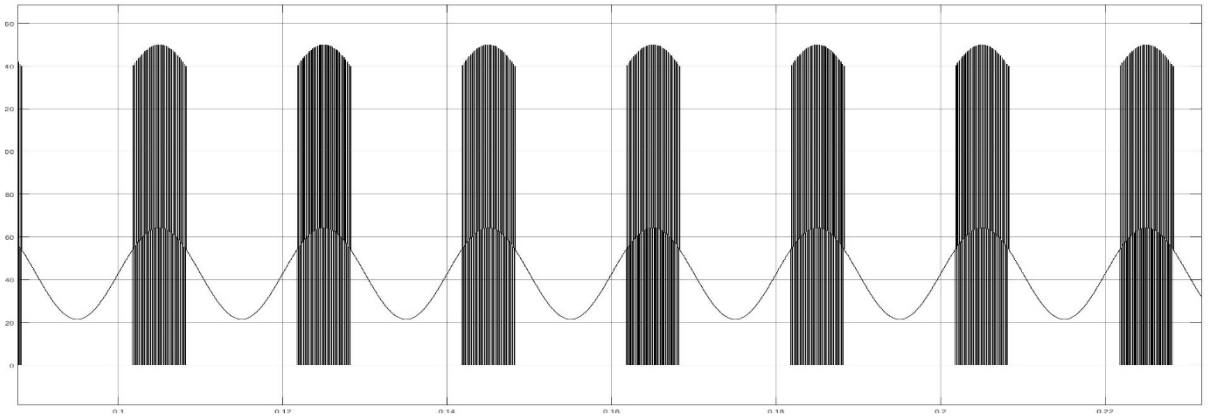

(b)

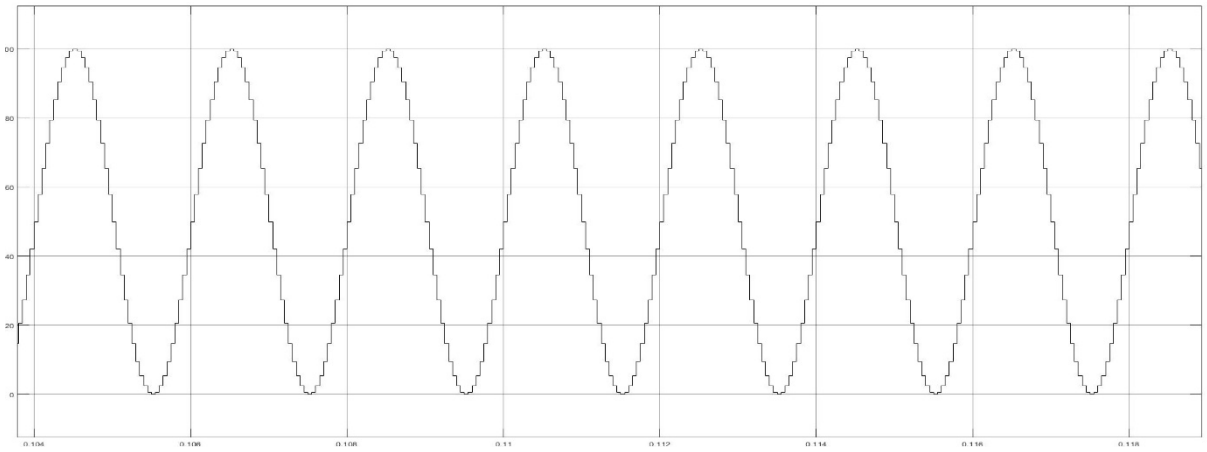

(c)

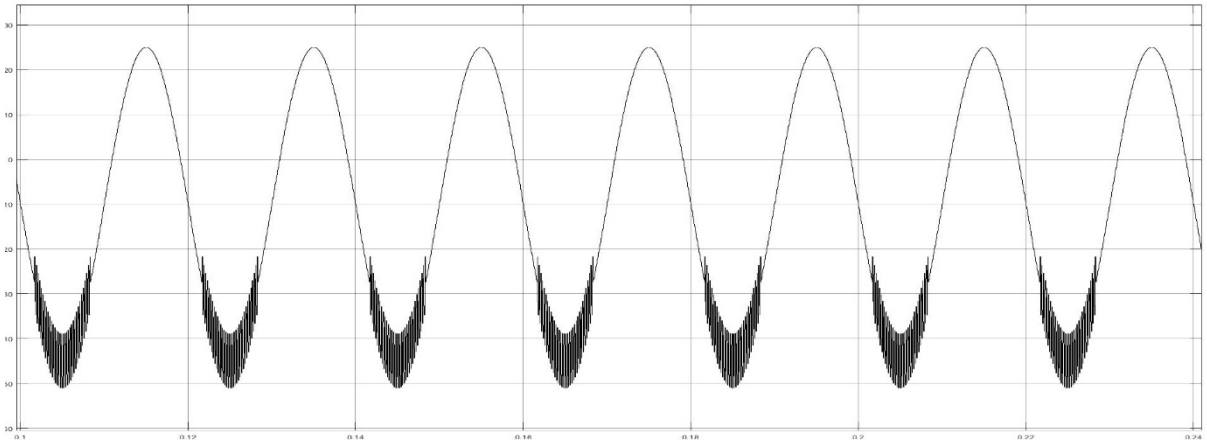

(d)

Fig 7: Single buck–boost cell operation for Uac = 230 VRMS operating with 16 A input phase current at 100 kHz. From top to bottom: ac- and dc-side half-bridge switchnode voltage (200 V/div), grid voltage (200 V/div), grid current (50 A/div) and inductor current (50 A/div).

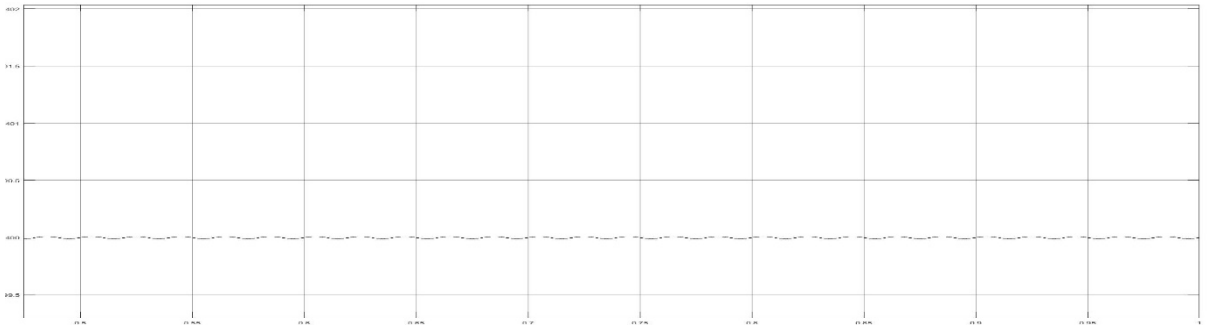

(a)

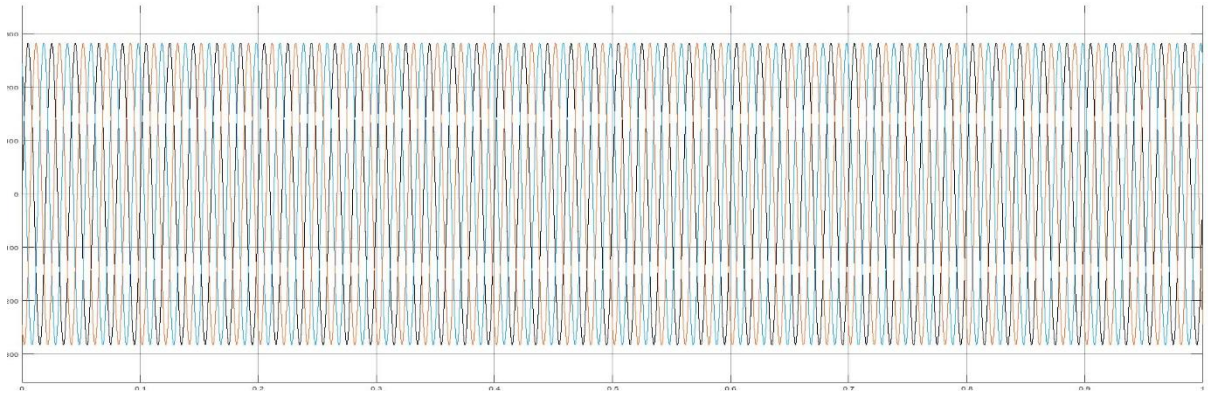

(b)

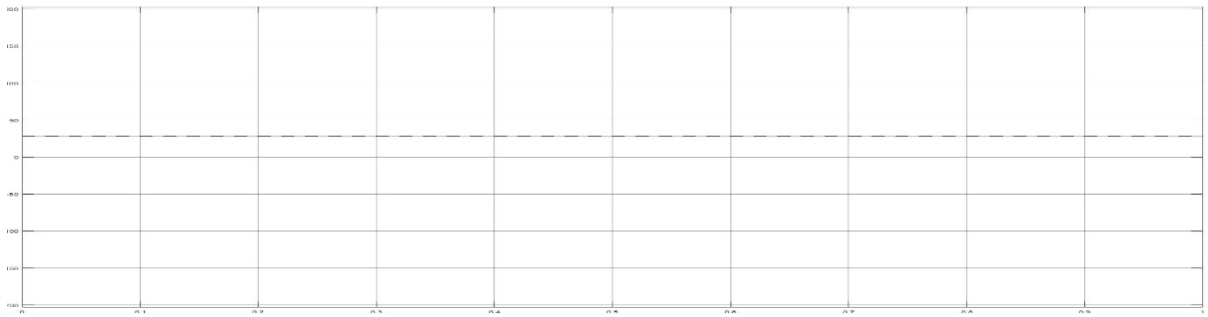

(c)

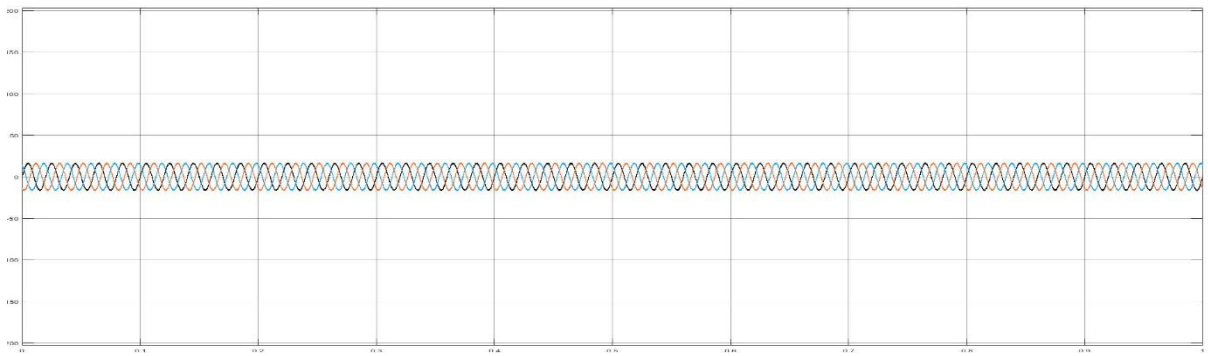

(d)

Fig 8: Three-phase operation for 400 VLL,rms, 11 kW. These rules are formulated based on expert knowledge or empirical data and follow linguistic logic, such as "IF temperature is high, THEN reduce power." The inference engine then processes these rules using logical operations like MIN-MAX or product inference methods to derive fuzzy outputs.

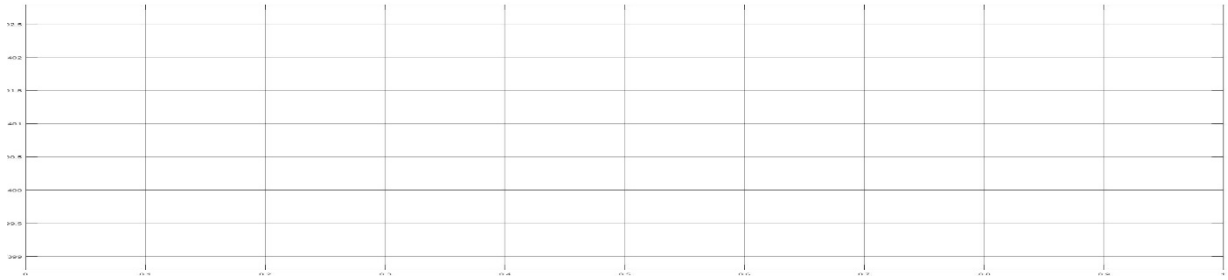

(a)

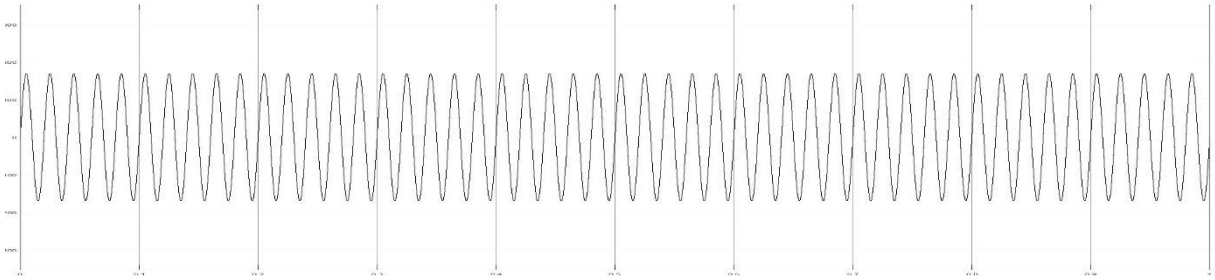

(b)

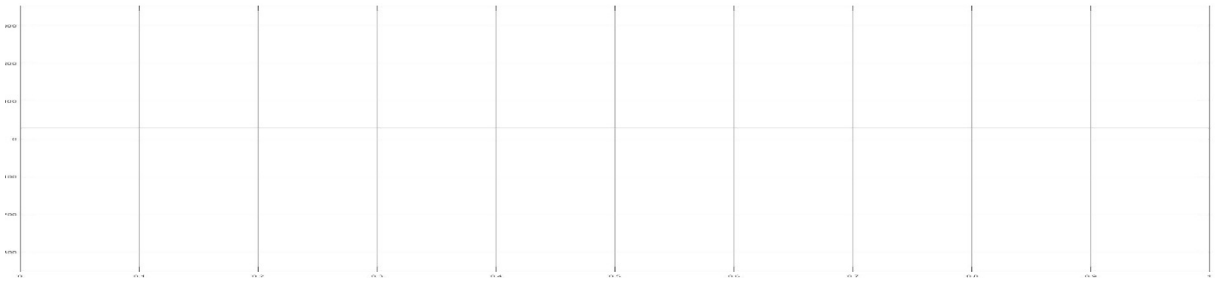

(c)

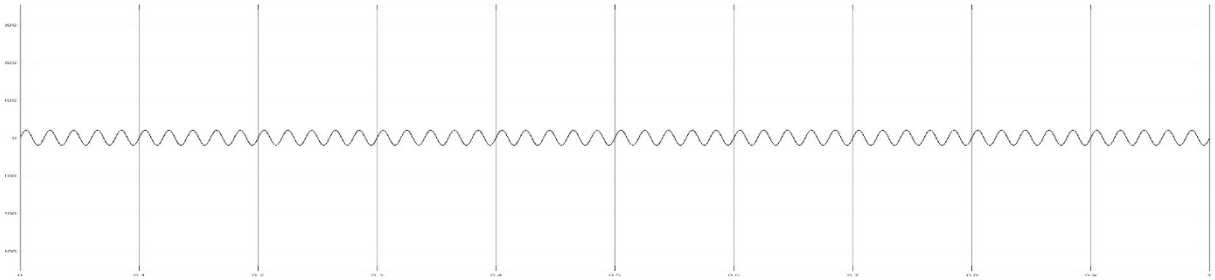

(b)

Fig 9 : Single-phase operation for 240 Vrms, 11 kW.

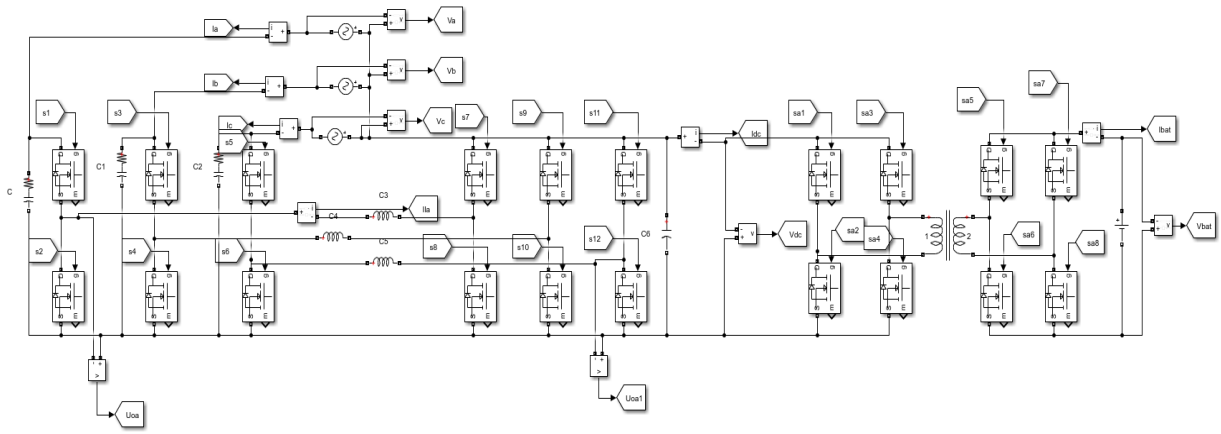

Fig 10: Three-phase operation for 400 VLL,rms, 11 kW circuit diagram of Bidirectional of ev on boarding charging

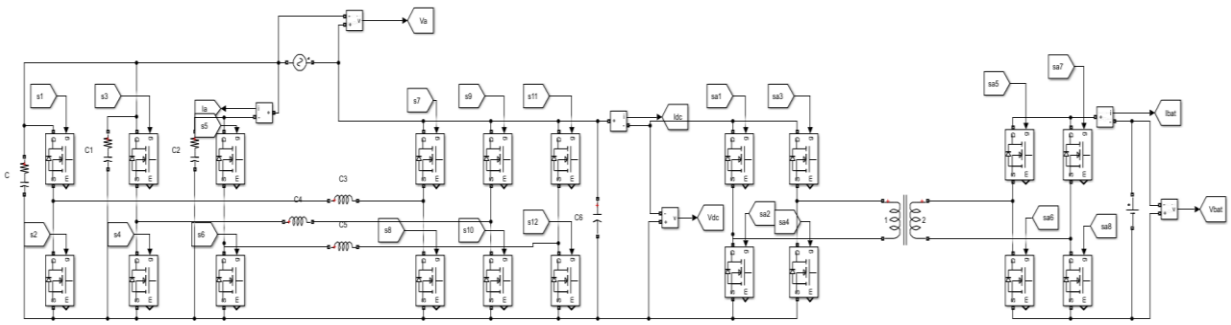

Fig 11: Single-phase operation for 240 Vrms, 11 kW circuit diagram of Bidirectional of ev on boarding charging

The final stage, defuzzification, converts the fuzzy outputs back into precise control signals, typically using methods like centroid, weighted average, or maximum membership. The FLC's ability to work with imprecise inputs and model human-like decision-making makes it highly applicable in various fields, including industrial automation, robotics, medical diagnosis, and consumer electronics. For example, in an air conditioning system, a fuzzy controller can adjust cooling levels smoothly based on room temperature and humidity instead of abrupt on-off switching, resulting in better comfort and energy efficiency. In the automotive industry, fuzzy logic is used in anti-lock braking systems (ABS) and automatic transmissions to ensure smooth gear shifting and optimal braking force. Another key application is in renewable energy systems, where FLCs optimize power output from solar panels and wind turbines by adjusting parameters dynamically based on environmental conditions. Compared to traditional PID controllers, which require precise mathematical models and struggle with system uncertainties, fuzzy logic controllers excel in handling nonlinear dynamics and disturbances. However, FLCs also have limitations, such as dependency on expert knowledge for rule formulation and challenges in tuning membership functions for highly complex systems. To address these issues, hybrid approaches integrating fuzzy logic with artificial intelligence techniques like neural networks and genetic algorithms have been developed, leading to self-adaptive and intelligent fuzzy controllers. With the rise of edge computing and the Internet of Things (IoT), FLCs are being increasingly deployed in embedded systems, enabling real-time intelligent decision-making in smart devices. Research is ongoing to enhance fuzzy logic systems with deep learning and reinforcement learning for advanced applications like autonomous vehicles and intelligent traffic control. The future of fuzzy logic controllers lies in their synergy with modern AI and computational intelligence techniques, driving innovation in automation and smart systems. Despite evolving technologies, fuzzy logic remains a powerful and intuitive approach for handling uncertainty, making it a valuable tool for engineers and researchers in developing robust and adaptive control solutions.

VI. CONCLUSION

To meet the demands of diverse operating conditions while ensuring compact and cost-effective designs, modern Electric Vehicles (EVs) increasingly depend on intelligent and high-efficiency On-Board Chargers (OBCs). As EV technology advances toward higher-voltage battery systems and sophisticated power flow regulation, new challenges arise—such as supporting seamless single- and three-phase operation, enabling bidirectional energy flow, and adapting to dynamic grid conditions. This article presents a novel fuzzy logic-based power conversion architecture for OBCs, integrating a Dual Active Bridge (DAB) DC-DC converter with a boost-type single-/three-phase front-end converter based on the buck-boost Y-rectifier. Unlike conventional systems, the proposed Fuzzy Logic Controller (FLC) offers enhanced adaptability by dynamically adjusting power conversion parameters in response to grid and battery variations.

By applying fuzzy logic, the system intelligently selects optimal control strategies using linguistic rules and membership functions, enabling smooth transitions between single- and three-phase modes

without requiring additional hardware or oversized components. The result is a real-time adaptive control mechanism that improves efficiency, stability, and responsiveness under fluctuating load and voltage conditions. The simplified control framework also reduces reliance on complex mathematical modeling and tuning procedures common in traditional PID-based systems, enhancing overall cost-effectiveness. To validate performance, an 11-kW bidirectional OBC prototype was tested across a wide range of conditions, consistently delivering efficient and stable operation throughout the output power range. Beyond improving power conversion and grid compatibility, the fuzzy logic-based approach supports bidirectional energy flow for vehicle-to-grid (V2G) applications—positioning it as a forward-looking solution for next-generation EV charging infrastructure.

REFERENCE

[1] H. Sarnago, O. Lucia, D. Menzi, and J. Kolar, "Single-/three-phase bidirectional EV on-board charger featuring full power/voltage range and a cost-effective implementation," in Proc. IEEE 17th Int. Conf. Compat., Power Electron. Power Eng., 2023, pp. 1–6.

[2] M. Yilmaz and P. T. Krein, "Review of battery charger topologies, charging power levels, and infrastructure for plug-in electric and hybrid vehicles," IEEE Trans. Power Electron., vol. 28, no. 5, pp. 2151–2169, May 2013.

[3] H.Sarnagoand, O.Lucía,"OptimizedEVon-boardchargingpowercon verter using hybrid DCX-DAB topology," in Proc. IEEE Appl. Power Electron. Conf. Expo., 2024, pp. 1305–1309.

[4] H. Wouters and W. Martinez, "Bidirectional onboard chargers for elec tric vehicles: State-of-the-art and future trends," IEEE Trans. Power Electron., vol. 39, no. 1, pp. 693–716, Jan. 2024.

[5] M.Y. Metwly, M. S. Abdel-Majeed, A. S. Abdel-Khalik, R. A. Hamdy, M. S. Hamad, and S. Ahmed, "A review of integrated on-board EV battery chargers: Advanced topologies, recent developments and opti mal selection of FSCW slot/pole combination," IEEE Access, vol. 8, pp. 85216–85242, 2020.

[6] S.Haghbin,S.Lundmark,M.Alakula,andO.Carls on,"Grid-connected integrated battery chargers in vehicle applications: Review and new solution," IEEE Trans. Ind. Electron., vol. 60, no. 2, pp. 459–473, Feb. 2013.

[7] A. Khaligh and M. D'Antonio, "Global trends in high-power on-board chargers for electric vehicles," IEEE Trans. Veh. Technol., vol. 68, no. 4, pp. 3306–3324, Apr. 2019.

[8] J. Yuan,L.Dorn-Gomba,A.D.Callegaro,J.Reimers, andA.Emadi,"A review of bidirectional on-board chargers for electric vehicles," IEEE Access, vol. 9, pp. 51501–51518, 2021.

[9] R. P. Upputuri and B. Subudhi, "A comprehensive review and per formance evaluation of bidirectional charger topologies for V2G/G2V operations in EV applications," IEEE Trans. Transp. Electrific., vol. 10, no. 1, pp. 583–595, Mar. 2024.

[10] H. Sarnago, O. Lucía, R. Jiménez, and P. Gaona, "High power density OBC featuring power pulsating buffer," in Proc. Int. Conf. Electric Electron. Hybrid Electric Veh. Elect. Energy Manage., 2021.

[11] H. Sarnago and O. Lucía, "Bidirectional 400-12 V dc-dc converter with improved dynamics and integrated transformer for EV applications," in Proc. IEEE Appl. Power Electron. Conf. Expo., 2024, pp. 3081–3085

[12] H. Sarnago, O. Lucia, R. Jiménez, and P. Gaona, "Differential-power processing on-board-charger for 400/800-V battery architectures using 650-V super junction MOSFETs," in Proc. IEEE Appl. Power Electron. Conf., 2021, pp. 564–568.

[13] B. Whitaker et al., "A high-density, high-efficiency, isolated on-board vehicle battery charger utilizing silicon carbide power devices," IEEE Trans. Power Electron., vol. 29, no. 5, pp. 2606–2617, May 2014.

[14] B. Li, Q. Li, F. C. Lee, Z. Liu, and Y. Yang, "A high-efficiency high density wide-bandgap device-based bidirectional on-board charger," IEEE Trans. Emerg. Sel. Topics Power Electron., vol. 6, no. 3, pp. 1627–1636, Sep. 2018. [Online]. Available: https://ieeexplore.ieee. org/document/8377992/

[15] P. Papamanolis, D. Bortis, F. Krismer, D. Menzi, and J. W. Kolar, "New EVbattery charger PFC rectifier front-end allowing full power delivery in 3-phase and 1-phase operation," Electronics, vol. 10, no. 17, 2021, Art. no. 2069.

[16] Y. Li, J. Schäfer, D. Bortis, J. W. Kolar, and G. Deboy, "Optimal synergetic control of a three-phase two-stage ultra-wide output voltage range EV battery charger employing a novel hybrid quantum series resonant DC/DC converter," in Proc. IEEE Workshop Control Model. Power Electron., 2020, pp. 1–11.

[17] T. Instruments, "GAN-based, 6,6-kw, bidirectional, onboard charger reference design," Texas Instruments, Rep. TI PMP22650, 2021.

[18] J. Lu et al., "A modular-designed three-phase high-efficiency high power-density EV battery charger using dual/triple-phase-shift con trol," IEEE Trans. Power Electron., vol. 33, no. 9, pp. 8091–8100, Sep. 2018.

[19] P. Papamanolis, D. Bortis, F. Krismer, D. Menzi, and J. W. Kolar, "New EVbattery charger PFC rectifier front-end allowing full power delivery in 3-phase and 1-phase operation," Electronics, vol. 10, no. 17, 2021, Art. no. 2069. [Online]. Available: https://www.mdpi.com/2079-9292/ 10/17/2069

[20] H. Sarnago, O. Lucia, S. Chhawchharia, D. Menzi, and J. W. Kolar, "Novel bidirectional universal 1-phase/3-phase-input unity power factor differential AC/DC converter," Electron. Lett., vol. 59, no. 13, 2023, Art. no. e12857. [Online].

[21] F. Krismer and J. W. Kolar, "Efficiency-optimized high-current dual active bridge converter for automotive applications," IEEE Trans. Ind. Electron., vol. 59, no. 7, pp. 2745–2760, Jul. 2012.

[22] M. Antivachis, D. Bortis, L. Schrittwieser, and J. W. Kolar, "Three phase buck-boost Y-inverter with wide DC input voltage range," in Proc. IEEE Appl. Power Electron. Conf. Expo., 2018, pp. 1492–1499.

[23] F.Krismerand, J.W.Kolar, "Closed form solution for minimum conduction loss modulation of DAB converters," IEEE Trans. Power Electron., vol. 27, no. 1, pp. 174–188, Jan. 2012.

[24] A. Darwish, A. M. Massoud, D. Holliday, S. Ahmed, and B. W. Williams, "Single-stage three-phase differential-mode buck-boost in converters with continuous input current for PV applications," IEEE Trans. Power Electron., vol. 31, no. 12, pp. 8218–8236, Dec. 2016.

[25] D.Menzi, M.Zhang, J.W.Kolar and J.Everts, "3-φ bidirectional buck boost sinusoidal input current three-level SiC Y-rectifier," in Proc. IEEE Appl. Power Electron. Conf. Expo., 2021, pp. 590–598.

[26] A. Mohamed, H. Shareef, A. Mohamed, and M. A. Hannan, "Fuzzy logic based charging algorithm for electric vehicles," *International Journal of Energy Research*, vol. 36, no. 6, pp. 630–643, 2012. DOI: 10.1002/er.1959

[27] S. Jain, N. S. Beniwal, and V. V. Tyagi, "Fuzzy logic controller for a bidirectional DC-DC converter in electric vehicle applications," *IEEE Int. Conf. on Power Electronics, Drives and Energy Systems (PEDES)*, 2014, pp. 1–6. DOI: 10.1109/PEDES.2014.7042082

[28] H. Mahmoudi, A. K. Adnan, and M. N. Aman, "Fuzzy logic based energy management system for hybrid electric vehicles," *Energy Reports*, vol. 6, pp. 1268–1279, 2020.

[29] T Lova Lakshmi, M Gopichand Naik & S. Rajendra Prasad. (2020). TLBO Algorithm for Multi-Level Inverter-Based Multi-Terminal HVDC System in Grid-Tied Photovoltaic Power Plant. Journal of The Institution of Engineers (India): Series B, Spinger, 435-442. https://doi.org/101.10.1007/s40031-020-00451-y